Mass conservation and anticorrelation effects in the colloidal aggregation of dense solutions

Marina Carpineti and Marzio Giglio
Dipartimento di Fisica, Università di Milano, via Celoria 16, 20133 Milano, Italy

Vittorio Degiorgio
Dipartimento di Elettronica, Università di Pavia, via Abbiategrasso 209, 27100 Pavia, Italy
(Received 13 June 1994)

Recent experimental data show that the scattered intensity distribution from dense solutions undergoing diffusion limited aggregation exhibits a peak at a nonzero wave vector. This article presents a simple phenomenological model based on the conjecture that the form factor for a realistic cluster should satisfy local mass conservation and hence exhibit a pronounced depression at zero wave vector. The model introduces two characteristic lengths, the cluster radius R_1 and the radius R_2 of the depletion region feeding the growing cluster, mass being conserved over the latter length. The intensity distributions observed during the initial stages of the aggregation process are interpreted on the basis of the form factor alone, while the description of the distributions in the later stages, in which scaling occurs, requires in addition the introduction of a structure factor which takes into account steric interactions among the clusters. The model shows remarkably good agreement with the experimental data, and also explains why earlier measurements on dilute solutions failed to exhibit the peak at a nonzero wave vector.

PACS number(s): 82.70.Dd, 81.10.Dn, 05.40.+J, 64.60.Cn

I. INTRODUCTION

In a recent paper [1] it has been shown that the scattered pattern from an aggregating colloidal system may exhibit a peak at a finite wave vector, very much like a separating system undergoing spinodal decomposition (SD). Such a feature is also present in a series of recent scattering experiments [2–9] on a variety of systems, all presenting an irreversible transition to a stable or time independent state which occurs via a coarsening process that eventually leads to the formation of stable phases. It should be mentioned that similar scattered intensity distributions are also observed in systems at equilibrium, such as the copolymer melts presenting the so-called "correlation hole" effect [10].

As it is well known, static light scattering has been widely used in connection with colloidal aggregation studies. One of the reasons for the success of static light scattering is undoubtedly associated with the easiness of the interpretation of the data and with the possibility of extracting, under the assumption of no interaction among aggregates, useful information such as the average aggregation number, the average radius of gyration, and the fractal dimension [11–13].

All the earlier scattering experiments on colloidal aggregation were performed on fairly dilute samples, and yielded scattered intensity distributions $I(q)$ showing their maximum value at $q=0$, q being the scattering wave vector, $q=4\pi\lambda^{-1}n\sin(\theta/2)$, where n is the index of refraction of the scattering medium, λ the wavelength in vacuum of the light beam, and θ the scattering angle. In the attempt of obtaining data on the late stages of aggregation, some of us [1] decided to investigate aggregation processes of smaller monomers, so that even at large aggregation numbers the relevant features of $I(q)$ would fall within the range of q values accessible to the low angle light scattering apparatus. Surprisingly, it was found [1] that $I(q)$ did exhibit a peak value I_m at a nonzero wave vector q_m, with I_m growing in the course of the aggregation process and q_m moving toward smaller and smaller values. Furthermore, the data of Ref. [1] show a very interesting scaling behavior of $I(q)$, somewhat similar to that observed in SD, which holds during the late stages of the aggregation process.

In this paper we present a simple model that quantitatively accounts for the results described in Ref. [1]. The model is mainly based on the approach used in Ref. [3] to explain the neutron scattering data on the kinetics of a crystal growth process, although additional ingredients are introduced here to improve the fit in the later stages of the aggregation. The physical origin of the peak of $I(q)$ lies in the fact that the aggregates grow by depleting a surrounding region of size R_2 larger than the aggregate size R_1. The quantity $R_2(t)$ represents the distance over which mass is actually fed by diffusion to the growing cluster of size $R_1(t)$, at the aggregation time t. Since the total number of monomers is conserved over a region of size $\geq R_2$, the scattered intensity has to be zero at $q=0$, and should remain low for 9 smaller than R_2^{-1}. Since the model and the fitting procedure introduce the two characteristic lengths R_1 and R_2 and other relevant parameters, relations between these quantities and their time evolutions will be derived.

The article is organized as follows. Section II recalls briefly the most relevant features of the experimental results. In Sec. III we describe in detail the model, including the definition of the two characteristic lengths. Section IV is devoted to the data analysis and to the discussion of the results of the fitting procedure.

II. EXPERIMENT

We recall that the experiments were performed with aqueous dispersions of polystyrene latex spheres with a radius of 9.5 nm, in the range of monomer concentrations 8.25×10^{13} cm$^{-3}\le c\le 8.25\times10^{14}$ cm^{-3} [1,14,15]. The aggregation was induced by adding $MgCl_2$ to the dispersion. The scattered intensity distributions were measured as a function of the aggregation time t by using a specially designed low-angle light scattering apparatus.

At fairly high salt content (8 mM $MgCl_2$) a peak in $I(q)$ appears as soon as data can be gathered during the course of the reaction [1]. While at earlier times the intensity distribution does not exhibit scaling properties, rather soon $I(q)$ can be scaled onto a unique master curve according to the scaling law

$$F(q/q_m)=q_m^{d_f}I(q/q_m)\ . \tag{1}$$

Ultimately the reaction stops when the close packing condition is reached. At such stage no further change in $I(q)$ occurs (it turns out that on a much longer time scale very slow restructuring phenomena are present, but we will ignore these processes here). If the monomer concentration is increased by keeping the salt concentration unchanged, the whole process develops at a faster rate, the most noticeable difference being now that the peak position during the reaction and at the final state is now shifted to larger q values, while the shape of $F(q/q_m)$ does not depend on the monomer concentration. Quite different is the effect of changes in the salt concentration c_s [14,15]. As c_s is reduced, in the initial stage of the reaction $I(q)$ does not exhibit any peak in the range of wave vectors accessible with our apparatus. Later on a peak eventually appears, and again its intensity grows in time and its position shifts to lower values of q, as shown in Fig. 1. Scaling behavior does occur only in the late stages of the reaction. If c_s is even further decreased, the peak makes its appearance at a much delayed time, and the scaling behavior is confined to the time interval just preceding the occurrence of close packing. Finally, typically at a salt content $c_s=2.5$ mM, the peak never appears before the close packing conditions are reached.

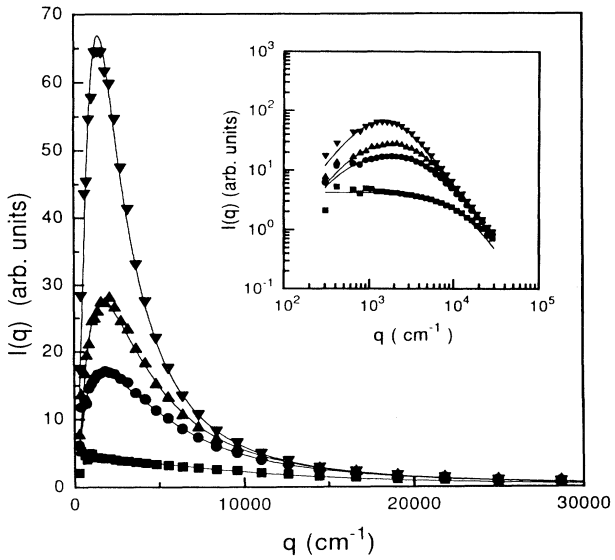

FIG. 1. Data collected at different times during the early stages of an aggregation performed with $c_0=4.37\times10^{14}$ cm^{-3} and 4 mM $MgCl_2$. The curves refer to the nonscaling regime only and the solid lines are fits of the experimental data with the form factor described in Eq. (7). In the inset a plot of the data on a log-log scale is shown.

In order to compare our phenomenological model with the experimental results, we have selected, among all the available data, those which are best suited to make evident the behavior in the various stages of the aggregation process. The data belonging to the nonscaling regime are obtained at intermediate salt content where they can be followed more easily. On the contrary, the scaling regime is studied in connection with data obtained at large c_s.

III. MODEL

We find it instructive to report on initial failures to attempt an interpretation of the scattered intensity distributions by following what seemed to be the most obvious way to proceed.

The form factor $P(q)$ commonly used to describe a fractal cluster is the Fisher-Burford (FB) distribution, originally proposed in the context of critical phenomena, which is given by [13]

$$P(q)=\frac{A}{\left[1+\dfrac{q^2R_g^2}{3d_f/2}\right]^{d_f/2}}\ , \tag{2}$$

where d_f is the fractal dimension, R_g the radius of gyration, and A is proportional to the weight average cluster mass M. Equation (2) can be derived by recalling that

$$P(q)\propto\int g(r)e^{iq\cdot r}d^3r \tag{3}$$

and by making the hypothesis that the correlation function $g(2)$ describing a fractal object has an expression similar to that used to describe critical fluctuations [16]:

$$g(r)\approx r^{d_f-3}\exp(-r\sqrt{3}/R_g)\ . \tag{4}$$

Actually, the FB form factor is the exact Fourier transform of Eq. (4) for $d_f=2$, while for $d_f\neq2$ Eq. (2) can be considered as an approximation to the exact formula [16]. Since in our case d_f is very close to 2, we will utilize here the FB form. At any rate, there is very convincing experimental evidence that the FB distribution does quite accurately describe the scattered intensity from fractal clusters in dilute solutions [17–19].

In the case of concentrated solutions the scattered intensity is no longer simply proportional to the form factor of the aggregates, but can be written as

$$I(q)\propto P(q)S(q)\ , \tag{5}$$

where $S(q)$ is the intercluster structure factor which takes into account the existence of correlations among

the mutual positions of the scattering objects. One could think at first that the observation of scattered intensities showing a peak at a nonzero wave vector and a pronounced depression at $q=0$ represents evidence of some kind of intercluster interaction, most likely of steric nature. This would suggest to interpret the experimental results with Eq. (5) by keeping the FB expression as the form factor and choosing an appropriate expression for the structure factor $S(q)$. Although the clusters have a rather diffuse boundary and a very tenuous bulk consistence, we selected a hard sphere (HS) structure factor obtained in the Percus-Yevick approximation. The obtained fits were not satisfying at all. Indeed, since the FB expression presents its maximum at $q=0$ where the experimental $I(q)$ is very close to 0, the fit imposes a $S(q)$ taking values close to 0 at $q=0$. This is possible for the HS structure factor only when the volume fraction is very large, in contrast with the experimental finding that $I(q)$ shows a well pronounced peak even in the early stages of aggregation when the clusters are small and very sparse.

We then decided to follow a different approach. In recent papers dealing with the growth of semiconductor nanocrystals in a glassy matrix [2,3] it was argued that the growth of the nanocrystal occurs at the expense of semiconductor material drawn from the region immediately surrounding the crystal. Therefore the semiconductor mass is conserved on the volume made up with the depletion volume and the crystal itself. We propose two almost equivalent schemes, based on the same mass conservation arguments, for the calculation of $I(q)$ associated with the growth of fractal aggregates. We want to point out that while for real HS systems it is very clear what the separate roles of the form factor and of the structure factor are, here, with fuzzily defined objects growing through the aggregation of neighboring objects, such a sharp distinction loses its meaning.

We start by considering the scattered intensity at the earlier stages of aggregation where the clusters are far apart and steric interactions can be neglected, so that $I(q)$ can be considered proportional to the form factor of the individual clusters. The very fact that $I(0)$ is close to zero implies, from Eq. (3), that the integral of $g(r)$ must vanish. Therefore, $g(r)$ must swing negative at some intermediate distance, or, in other words, some kind of anticorrelation is established at that range. While the inner positive part of $g(r)$ accounts for the cluster's denser core, the negative contribution at larger r is associated with the depletion region.

The first scheme attempts to give an analytical expression to the form factor of the scattering object represented by cluster plus depletion volume, by starting from a realistic form for the pair correlation function $g(r)$. The function $g(r)$ must have the following features: (i) it must account for the fractal morphology clearly evident from the high q region of the scattering plots shown in Fig. 1; (ii) it must exhibit an anticorrelation effect so that its integral should vanish; (iii) it must present the possibility of a scaling behavior. The simplest form satisfying all these constraints is given by the difference between two functions having the same structure as that shown in Eq. (4):

$$g(r)=g_1(r)-g_2(r)\approx r^{d_f-3}\left[\frac{1}{R_1^{d_f}}\exp\left[-\frac{r\sqrt{3}}{R_1}\right]-\frac{1}{R_2^{d_f}}\exp\left[-\frac{r\sqrt{3}}{R_2}\right]\right], \tag{6}$$

where R_1 and R_2 are the inner cluster core and depletion region radii (clearly, R_2 is larger than R_1), and the factors multiplying the exponentials are inserted to ensure that the volume integral of $g(r)$ vanishes. With this model R_1 is proportional to R_g. Note that r presents a lower cutoff at a value corresponding to the monomer radius r_0 and that the use of Eq. (6) implies that $r_0 \ll R_1$.

We present in Fig. 2 a plot of $g(r)$ evaluated for a ratio $R_2/R_1=3$. The plot in the main figure is on a highly expanded vertical scale, and the distances on the linear horizontal scale are reported in units of $x=r/r_0$ (we have chosen $R_1=100r_0$). The position of the smallest attainable scaled distance $x=1$ cannot be appreciated, and for small values of x the curve is off scale. The main purpose for showing this plot is to point out how shallow the negative minimum actually is. The same curve is redrawn in the inset where now the x axis is in a logarithmic scale, the vertical scale being compressed so that the value of the correlation function at $x=1$ does appear on the plot. Notice that on this scale the minimum is not visible at all. Yet the correlation function does have zero volume integral. The fact that the minimum is so shallow in Fig. 2 could probably explain why three-dimensional (3D) simulations have not produced evidence of the existence of a negative part of $g(r)$ [20]. Indeed the statistical accuracy needed to observe the shallow minimum can probably be attained only by extremely large scale simulations. For

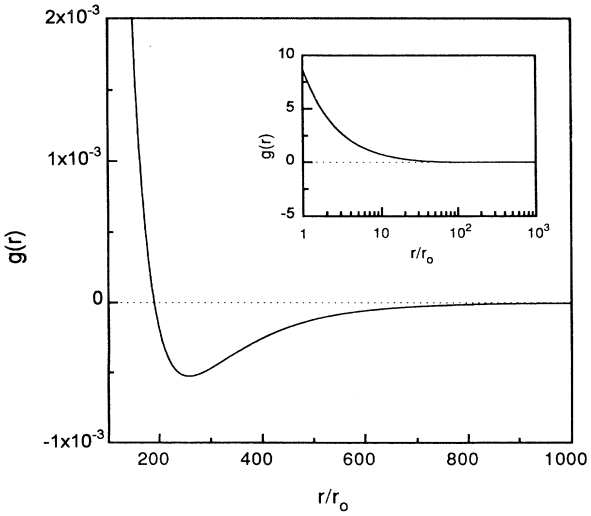

FIG. 2. Sketch of the correlation function $g(r)$ [see Eq. (6)] as a function of r/r_0. $g(r)$ is evaluated for a ratio $R_1/R_2=3$, and for $r_0=R_1/100$. The same curve is redrawn in the inset over a more compressed vertical scale and with the x axis on a log scale.

the same reason it is likely that direct 3D observations via, e.g., confocal microscopy will be equally doomed to failure (they would also require larger monomers). At variance, low-angle light scattering is ideally suited for this job, since mass conservation implies large effects at low q and statistical averaging is excellent.

The approximate form factor derived from Eq. (6) reads

$$P(q)=\frac{A}{\left[1+\frac{q^2R_1^2}{3d_f/2}\right]^{d_f/2}}-\frac{A}{\left[1+\frac{q^2R_2^2}{3d_f/2}\right]^{d_f/2}} . \quad (7)$$

Equation (7) is the simplest modification of the commonly used FB expression which accounts for the presence of a peak at a nonzero wave vector, giving at the same time zero scattered intensity at $q=0$ [21] and the correct behavior at large q.

The second approach we have followed starts from the consideration that, in the case of a scattering object which is not pointlike, the scattered field is given by the addition of all the fields scattered by the different subvolumes with the appropriate amplitude and phase, and the scattered intensity is calculated by taking the modulus square of the field. In our case, we describe the scattering object by a continuous deterministic function $\delta(r)$ which represents the local deviation from the average concentration of dispersed material. We put $\delta(r)=\delta_1+\delta_2(r)$, where $\delta_1(r)$ is the positive contribution due to the inner core, and $\delta_2(r)$ is the negative contribution due to the depleted region. The mass conservation constraint requires that the volume integral of $\delta(r)$ be equal to zero. This approach would lead us to write, instead of Eq. (7), the following expression for $P(q)$:

$$P(q)=[F_1(q)+F_2(q)]^2 , \quad (8)$$

where

$$F_j(q)=\int 4\pi r^2\delta_j(r)\frac{\sin(qr)}{qr}dr . \quad (9)$$

Since, at large q, $P(q)$ goes as $[F_1(q)]^2$, it is reasonable to assume that $[F_1(q)]^2$ coincides with the FB distribution given in Eq. (2). If we also now assume that $[F_2(q)]^2$ is given by a FB distribution, we end up with the following expression for $P(q)$:

$$P(q)=\left\{\left[\frac{A}{\left[1+\frac{q^2R_1^2}{3d_f/2}\right]^{d_f/2}}\right]^{1/2}-\left[\frac{A}{\left[1+\frac{q^2R_2^2}{3d_f/2}\right]^{d_f/2}}\right]^{1/2}\right\}^2 . \quad (10)$$

We have found that the experimental data can be described equally well by the two form factors presented in Eq. (7) and Eq. (10). The trends followed by the fitting parameters are quite similar for the two models, the main difference being that the second model gives larger numerical values for R_2. Since the results obtained in the two cases are very similar, we will only discuss in detail the data interpretation based on the first model.

As we shall see, the form factor alone is not sufficient to describe $I(q)$ during the entire duration of the aggregation reaction. In fact, when the close packing condition is approached, intercluster interactions have to be considered. To do so, we have chosen a structure factor that accounts for steric interactions only. For the sake of simplicity, we use the hard sphere structure factor with R_1 as the hard sphere radius. There are various reasons why our choice could be somewhat inadequate. First, the fractal aggregates are tenuous inside and have fuzzy boundaries. Second, the system is very likely polydisperse, and the approximation used might not be very accurate [22]. However, at the present stage of development of our phenomenological model, it is probably unnecessary to introduce a too detailed description of $S(q)$.

IV. DATA ANALYSIS

As it was pointed out above, the data presented in Fig. 1 refer to the initial stages of an aggregation process induced in a dispersion containing 4 mM $MgCl_2$. We found that, in this stage, the data are well described by using the form factor alone, and keeping the structure factor identically equal to 1. The full lines in Fig. 1 represent the best fit obtained by using the form factor of Eq. (7). For simplicity, we have kept constant the fractal dimension at the value $d_f=2$, so that the fit procedure yields only the three parameters R_1, R_2 and A.

In the later aggregation stage, the data are better described by Eq. (5), where the form factor is still given by Eq. (7) and the structure factor is the hard sphere one $S_{HS}(qR_1,\Phi)$ which is a function of the product qR_1 and of the volume fraction Φ [23]. We show in Fig. 3 the best

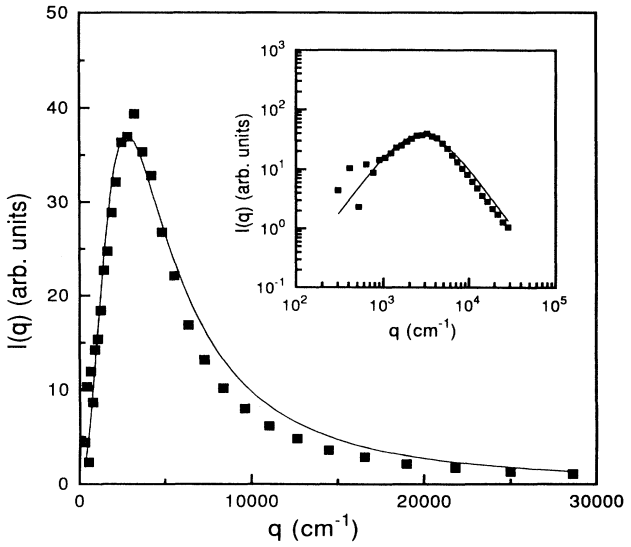

FIG. 3. Fit of an experimental curve in the scaling regime performed with the form factor alone [see Eq. (7)]. The data have been collected during the late stages of an aggregation performed with $c_0=4.37\times10^{14}$ cm^{-3} and 6 mM $MgCl_2$.

fit to a scattering distribution which was gathered in the time domain where scaling of $I(q)$ does hold, during an aggregation run at 6 mM $MgCl_2$. The full line is an attempt to fit the data with the form factor alone. As one can notice, the fit is poor. In Fig. 4 we show a fit to the same data in which both form factor and structure factor are used. The fit is now very good. In the figure, we show the two separate contributions due to $P(q)$ and $S_{HS}(q)$. One can notice that even for the case shown here, the structure factor contribution to the overall behavior is not very pronounced.

A first important conclusion suggested by the fit is that the presence of the peak in $I(q)$ and the fact that $I(0)=0$ are basically due to mass conservation applied to the volume enclosing the cluster plus its depletion region, and do not necessarily imply any ordering in the spatial arrangement of clusters.

From the fitting procedure we can derive the time evolution of the four parameters R_1, R_2, A, and Φ. We show in Fig. 5 the time evolution of R_1 and R_2, and in Fig. 6 the time evolution of the ratio R_2/R_1. In both figures the arrow indicates the time t_s around which the transition from nonscaling to scaling behavior occurs. The inner core radius R_1 grows as a function of time, as expected since the cluster size does increase during the aggregation process. The behavior of R_2 is more complex. The data show that it actually decays at first, reversing this trend when the scaling behavior sets in. The size of the depletion region is essentially controlled by diffusion processes. Initially the clusters grow by aggregating monomers which have large diffusion coefficients and can therefore diffuse over large distances in a given time interval. When the clusters become larger, growth is mainly due to cluster-cluster aggregation. The diffusing

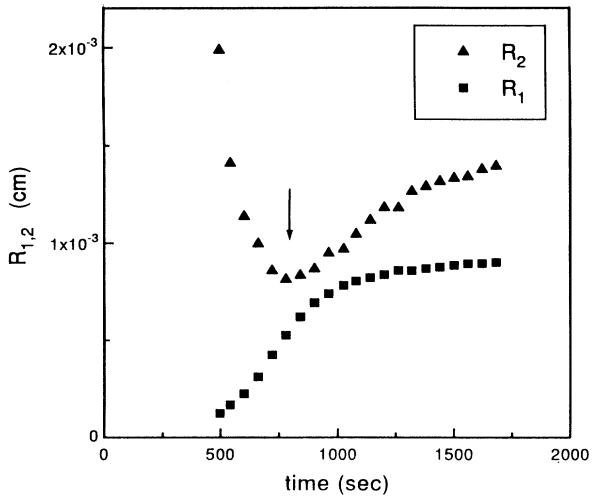

FIG. 5. Time evolution of the two radii R_1 and R_2 for a measurement performed with $c_0=4.37\times10^{14}$ cm^{-3} and 6 mM $MgCl_2$. The arrow indicates the transition from nonscaling to scaling behavior.

species have small diffusion coefficients, and this reduces the effective size of the depletion region. To put this matter in a more quantitative way, we recall that the cluster mass M grows according to the law

$$\frac{dM}{dt}=JR_1^2 , \tag{11}$$

where J is the mass flow, and we have assumed that all the clusters which cross the surface enclosing the growing cluster do form a bond. J is given by Fick's law,

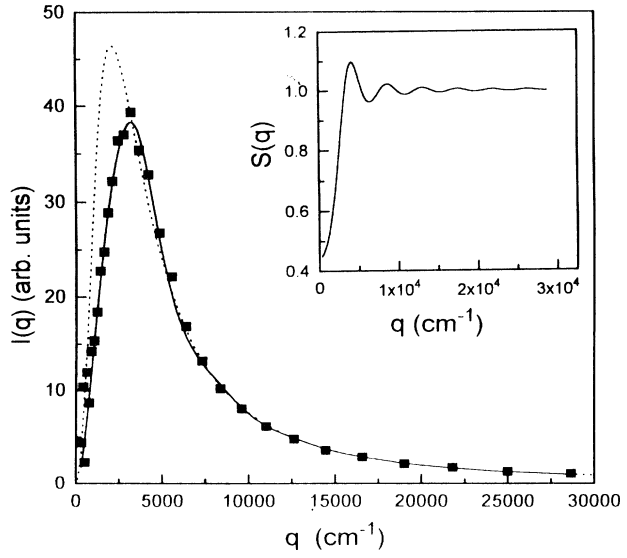

FIG. 4. Fit of the same curve shown in Fig. 3 by means of $I(q)=P(q)S(q)$ (solid line). The contributions of $P(q)$ and $S(q)$ are shown separately. $S(q)$ is shown in the inset, while $P(q)$ is the dotted line.

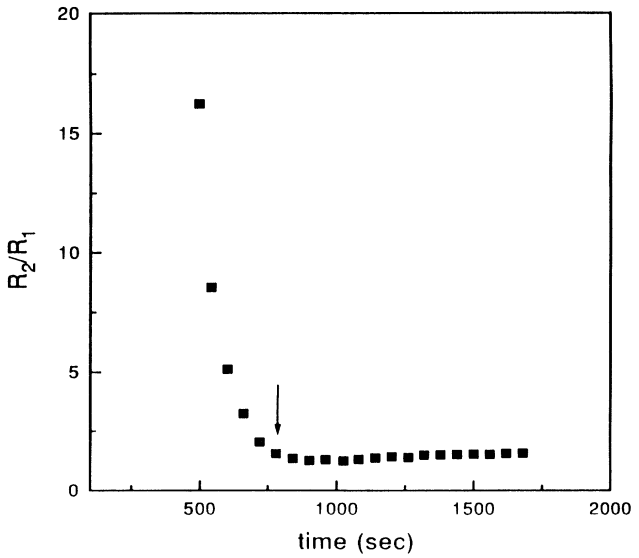

FIG. 6. Time evolution of the ratio R_2/R_1 for the same measurement of Fig. 5. Again, the arrow indicates the transition from nonscaling to scaling behavior.

$J=-\rho D\ \mathrm{grad}(c)$, where ρ is the number density and D the diffusion coefficient. Here $\rho \approx \rho_0/R_1^2$ where ρ_0 is the monomer concentration and the fractal dimension is taken equal to 2, and D is inversely proportional to R_1. For a diffusion limited aggregation process it is known that the mass should grow linearly with time, that is, dM/dt is constant. The size R_2 of the depletion region can then be estimated form the value of grad(c) at the cluster surface. The steeper grad(c) is, the shorter the distance R_2 beyond which the presence of a growing cluster is not felt by the bulk solution. From the previous considerations we find that

$$\mathrm{grad}(c)|_{r=R_1} \approx R_1/\rho_0 \ . \tag{12}$$

In spite of the crudeness of the model, this relation accounts for two important facts. First, as the cluster grows, grad(c) gets larger, and therefore the radius R_2 becomes smaller. Second, the actual value of R_2 depends on the initial monomer concentration and it is larger at lower values of ρ_0. The fact that the ratio R_2/R_1 comes out to be inversely proportional to ρ_0 is very interesting and can explain why previous experiments, performed at much lower values of ρ_0 than those discussed here, have failed to see the low q depression of $I(q)$. Note that the form factor of Eq. (7) presents a maximum at a value q_m given by

$$q_m = \frac{\sqrt{3}}{R_1}\left[\frac{R_1}{R_2}\right]^{1/2} \ . \tag{13}$$

If the ratio R_2/R_1 is large, the maximum is shifted, at fixed R_1, to very small angles, well outside the experimentally accessible range. This explains the experimental evidence that the peak never appears if the salt content is sufficiently reduced [14]. In fact, in the slow aggregation mode, monomers can diffuse over larger distances as a consequence of the small sticking probability, so that the ratio R_2/R_1 is large at any aggregation rate. In the scaling regime, the behavior of R_2 closely follows that of R_1, as it is evidenced by the fact that the ratio R_2/R_1, after the initial decay, levels off at a constant value around 1.45 (see Fig. 6). It should be noted that scaling rigorously implies that the ratio R_2/R_1 should remain constant. As pointed out before, this ratio changes rather rapidly during the early nonscaling phases. In this regard we want to stress that the fitting of the scattering distributions in the early phases requires only three floating parameters, and the statistical accuracy of the estimates of R_1 and R_2 is at least as good as in the late scaling regime. Indeed if one attempts to fit the early data by constraining the ratio R_2/R_1 to the constant value observed in the scaling regime ($R_2/R_1 \approx 1.45$), the quality of the fitting becomes definitely poor.

We present in Fig. 7 the behavior of the best-fit parameters A and Φ versus the aggregation time. In the nonscaling region, that is, for $t < t_s$, the parameter A, which is proportional to M, grows with time in a way consistent with the law: $A \propto R_1^2$. This is what is expected from fractal aggregates having a fractal dimension close to 2. We have no model for the observed behavior of A for

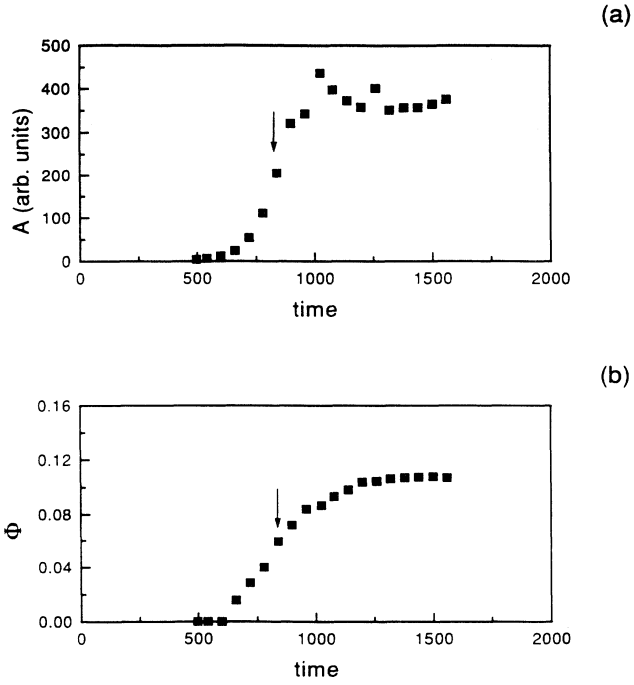

FIG. 7. Growth of the best fit parameters A (a) and Φ (b) for a measurement performed with $c_0 = 4.37 \times 10^{14}$ cm^{-3} and 6 mM $MgCl_2$.

$t > t_s$. It should be noted, in any case, that the best-fit values of A in the scaling regime may be strongly influenced by small changes of the structure factor $S(q)$, so that the values obtained in this regime should be treated with some caution. The volume fraction Φ is also growing with t, leveling off in the scaling regime, as expected.

As noted above, we have neglected polydispersity effects. In principle, if the size distribution is known, it is possible to generalize our model. In the dilute dispersion regime, where interactions are negligible, $I(q)$ is simply a weighted average of form factors of clusters of different sizes. Since each form factor is a peaked function starting with zero value at $q=0$, also $I(q)$ will be zero at $q=0$ and will present a peak at a finite wave vector. The effect of polydispersity will be that of introducing a smoothing in the shape of $I(q)$. When interactions are non-negligible, the fit becomes difficult because no analytical solutions are available for the structure factor of a polydisperse system. However, one can say that, qualitatively, the effect should be again that of smoothing the shape of $I(q)$, still preserving the depression at small q values. It should be noted that most of the results discussed in this article refer to situations close to the diffusion-limited aggregation regime where a large polydispersity in cluster size is not expected.

Finally, we must stress that all the data that we have analyzed (only a small fraction of them is presented here) do show an encouraging degree of consistency and all the runs performed at various concentrations exhibit the same trends.

As a conclusion, we have shown in this work that a model based on a local mass conservation criterion can explain the scattered intensity distributions observed in low-angle static light scattering experiments on aggregation processes in dense colloidal dispersions [24]. The mass conservation criterion implies, by itself, that the scattered intensity should be zero at zero scattering angle and should present a peak at a nonzero wave vector, irrespective of any correlation which might exist among the mutual positions of clusters. We have proposed a specific form for the intracluster correlation function $g(r)$ which is only based on heuristic arguments. The chosen form fits very well the data obtained in the earlier stages of aggregation, whereas the description of the scaling regime requires the introduction of an additional ingredient, an intercluster structure factor. Some of the specific choices we have made for the fitting functions are rather arbitrary, and there is clearly a need for a firmer theoretical basis. The visibility of the peak in a real experiment is connected with the fact that the peak position q_m should fall in the experimentally accessible range of wave vectors. Our model provides an explanation for the fact that earlier scattering experiments on colloidal aggregation have failed to observe the peak in $I(q)$.

ACKNOWLEDGMENTS

We thank L. Reatto and R. Klein for useful comments. We acknowledge financial support from the Italian Ministry for University and Research (MURST 40% funds). Two of us (M.C. and M.G.) acknowledge financial support from ASI (Agenzia Spaziale Italiana).

[1] M. Carpineti and M. Giglio, Phys. Rev. Lett. **68**, 3327 (1992).
[2] V. Degiorgio, G. P. Banfi, G. Righini, and A. R. Rennie, Appl. Phys. Lett. **57**, 2879 (1990); A. R. Rennie, V. Degiorgio, and G. P. Banfi, Physica B **180 & 181**, 589 (1992).
[3] G. P. Banfi, V. Degiorgio, A. R. Rennie, and J. G. Barker, Phys. Rev. Lett. **69**, 3401 (1992).
[4] K. Schätzel and B. J. Ackerson, Phys. Rev. Lett. **68**, 337 (1992).
[5] J. Bibette, T. G. Mason, H. Gang, and D. A. Weitz, Phys. Rev. Lett. **69**, 981 (1992).
[6] M. D. Haw, W. C. K. Poon, and P. N. Pusey, Physica A **208**, 8 (1994).
[7] D. J. Robinson and J. C. Earnshaw, Phys. Rev. Lett. **71**, 715 (1993).
[8] D. Beysens, and C. M. Knobler, Phys. Rev. Lett. **57**, 1433 (1986).
[9] P. W. Rouw, A. T. J. M. Woutersen, B. J. Ackerson, and C. J. De Kruif, Physica A **156**, 876 (1989).
[10] P. G. de Gennes, in *Scaling Concepts in Polymer Physics* (Cornell University Press, Ithaca, NY, 1985).
[11] D. W. Schaefer, J. E. Martin, P. Wiltzius, and D. S. Cannell, Phys. Rev. Lett. **52**, 2371 (1984).
[12] M. Y. Lin, H. M. Lindsay, D. A. Weitz, R. Klein, R. C. Ball, and P. Meakin, J. Phys. Condens. Matter **2**, 3093 (1990).
[13] M. Y. Lin, R. Klein, H. M. Lindsay, D. A. Weitz, R. C. Ball, and P. Makin, J. Colloid Interface Sci. **137**, 263 (1990).
[14] M. Carpineti and M. Giglio, Phys. Rev. Lett. **70**, 3828 (1993).
[15] M. Carpineti and M. Giglio, J. Phys. Condens. Matter **6**, 329 (1994).
[16] See, for example, S. K. Sinha, Physica D **38**, 310 (1989).
[17] G. Dietler, C. Aubert, D. S. Cannell, and P. Wiltzius, Phys. Rev. Lett. **57**, 3117 (1986).
[18] M. Carpineti, F. Ferri, M. Giglio, E. Paganini, and U. Perini, Phys. Rev. A **42**, 7347 (1990).
[19] D. Asnaghi, M. Carpineti, M. Giglio, and M. Sozzi, Phys. Rev. A **45**, 1018 (1992).
[20] P. Meakin (private communication).
[21] It should be noted that, rigorously speaking, $I(0)$ is not equal to zero, but it should coincide with the intensity scattered by the dispersion of unaggregated monomers, that is, with the value $I(0)$ presented at $t=0$. However, such an intensity is much smaller than the values observed on the aggregating dispersion, so that, for practical purposes, it can be set equal to 0.
[22] R. Klein, in *Structure and Dynamics of Strongly Interacting Colloids and Supramulecular Aggregates in Solution,* Vol. 369 of *NATO Advanced Study Institute, Series C: Mathematical and Physical Science,* edited by S. H. Chen, J. S. Huang, and P. Tartaglia (Kluwer, Dordrecht, 1992), pp. 39–96.
[23] See, for example, J. P. Hansen and I. R. Mc Donald, *Theory of Simple Liquids* (Academic, London, 1986).
[24] While this manuscript was in preparation, we received a report by F. Sciortino and P. Tartaglia dealing with the same problem.